Drug Development and Industrial Pharmacy, 34:683–691, 2008

ISSN: 0363-9045 print / 1520-5762 online
DOI: 10.1080/03639040701836636

informa
healthcare

Physicochemical Properties of the Nucleoside Prodrug R1626 Leading to High Oral Bioavailability

Michael Brandl, Xiaoyang Wu, Marites Holper, Lei Hong, Zhongjiang Jia, Raj Birudaraj, Micaela Reddy, Tom Alfredson, Tony Tran, Susan Larrabee, Xu Hadig, Keshab Sarma, Carla Washington, George Hill, and David B. Smith
Roche Palo Alto, Palo Alto, CA, USA

The nucleoside analog R1479 is a potent and highly selective inhibitor of NS5b-directed hepatitis C virus (HCV) RNA polymerase in vitro. Because of its limited permeability, lipophilic prodrugs of R1479 were screened. Selection of the prodrug involved optimization of solubility, permeability, and stability parameters. R1626 has dissociation constant, intrinsic solubility, log partition coefficient (*n*-octanol water), and Caco-2 permeability of 3.62, 0.19 mg/mL, 2.45, and 14.95×10^{-6} cm/s, respectively. The hydrolysis of the prodrug is significantly faster in the Caco-2 experiments than in hydrolytic experiments, suggesting that the hydrolysis is catalyzed by enzymes in the cellular membrane. Using GastroPlus™, the physical properties of R1626 successfully predict the dose dependence of the pharmacokinetics in humans previously studied. The program predicts that if the particle size of R1626 is less than 25 μm, it will be well absorbed. Prodrugs with a solubility of greater than 100 μg/mL and permeability in the Caco-2 assay greater than 3×10^{-6} cm/s are expected to achieve a high fraction absorbed.

Keywords prodrug; nucleoside; physicochemical properties; R1626

INTRODUCTION

Optimization of the physicochemical properties of drug candidates to improve oral bioavailability is vital in the drug selection process (Avdeef, 2001; Di & Kerns, 2006; Hageman, 2006; Ho, Park, Morozowich, & Higuchi, 1976; Ungel & Abrahamsson, 2001). Prodrugs (Albert, 1958) are a common approach to improve the physical properties and overcome the barriers to oral absorption (Beaumont, Webster, Gardner, & Dack, 2003; Cho, 2006; Gomez-Orellana, 2005; Mackman & Cihlar, 2004; Stanczak & Ferra, 2006; Stella, 2006; Stella, Charman, & Naringrekar, 1985). Because of the hydrophilic nature and the resulting low permeability of many nucleoside and nucleotide drugs, they are frequently considered as candidates for prodrug formation (Li, Maag, & Alfredson, in press; Poijärvi-Virta & Lönnberg, 2006). For prodrugs that seek to increase passive permeability, such as oseltamir, zanamivir, and famciclovir, obtaining the right balance of lipophilicity and solubility can be challenging and is of importance in selection of a successful drug candidate (Ettmayer, Amidon, Clement, & Testa, 2004; Stella, 2007).

Hepatitis C virus (HCV) infection is a leading cause of liver diseases such as cirrhosis and hepatocellular carcinoma. Nucleoside and nucleotide inhibitors for the treatment of HC are in various stages of development (Shim, Hong, & Wu, 2006). The nucleoside analog R1479 (4′-azidocytidine) is a potent and highly selective inhibitor of NS5b-directed HCV RNA polymerase in vitro (Devos et al., 2002; Klumpp et al., 2006). Optimization of the physicochemical properties of the drug to improve the bioavailability resulted in the selection of the tri-isobutyrate prodrug, R1626 (Alfredson et al., 2006; Li, Maag, & Alfredson, in press; Smith et al., 2006). The prodrug has shown high blood plasma levels of the parent compound and low levels of the potential mono- and diester analogs in single ascending dose studies from 500 to 12,000 mg (Robson et al., 2007). Furthermore, the prodrug has shown robust antiviral activity, in monotherapy in chronic HCV patients (Roberts et al., 2006). In this article, the physicochemical properties of the hydrochloride salt of R1626 are reported, and GastroPlus™ software was used to understand the relationship between the key pharmaceutical properties of prodrugs of R1479 and the extent of absorption. The analysis shows that alkyl ester prodrugs of nucleosides that improve passive permeability can have a high oral bioavailability by obtaining the optimum balance of lipophilicity and solubility.

MATERIALS AND METHODS

Materials

The crystalline hydrochloride salt of R1626, R1626 (free base), a mixture of the 2′- and 3′-monoisobutyrate esters, the 5′-monoisobutyrate ester, 2′-3′-di-isobutyrate ester, and R1479 hemi-sulfate were prepared by Chemical Development, Roche Palo Alto (Palo Alto, CA, USA). All other reagents were of analytical grade.

Address correspondence to Michael Brandl, Roche Palo Alto, LLC, 3431 Hillview Avenue, Palo Alto, CA 94304, USA. E-mail: michael.brandl@roche.com

pH Determination

pH measurements were taken at room temperature using an Orion Triode™ pH meter (model 611; Thermo Scientific, Waltham, MA) electrode calibrated with aqueous standard buffer solutions. pH values have not been corrected for temperature.

Dissociation Constant

The dissociation constant of R1626 was determined at 25.0 ± 0.5°C and 0.15 M (KCl) ionic strength using the Sirius GLpKa titrator (Sirius Analytical Instrument Ltd., East Sussex, UK). The GLpKa titrator was controlled by GLpKaControl (version 1.005). Approximately 3–4 mg of the compound was weighed into four titration vials; 18 mL of 0.15 M (KCl) aqueous solution was added to each vial. The titration assays were performed from pH 2.0 to 10 under argon atmosphere using standardized 0.5 M HCl and 0.5 M KOH as titrants. A difference curve of average number of bound protons versus pH was derived by subtracting the blank titration curve (titration in 20 mL 0.15 M KCl aqueous solution only) from the sample titration curve. The titration data were uploaded from the GLpKa titrator to a computer and refined by the pKaLOGP software (version 5.2a) using "goodness-of-fit" (GOF).

Solubility Determination

For solubility in water, excess of R1626 was added to 4 mL of solvent in glass vials with Teflon-lined screw caps. The samples were tumbled (at 25 rpm) for 1–5 days in the solubility bath maintained at 25°C. At selected time intervals, sample suspensions were centrifuged, and the solutions were diluted and assayed by high-performance liquid chromatography (HPLC).

The pH-solubility measurements were made by adding approximately 1.0 g of drug to 10 mL of water to form a suspension. Samples were vortexed and left to sit for at least 20 min before measuring the pH value, then the sample was filtered through a 0.45-μm Pall Gellman Acrodisc filter and diluted with 50% acetonitrile before analysis by using HPLC. The drug suspension was then titrated with 1.0 M KOH to raise the pH. Again, the suspensions were vortexed and left to sit for at least 20 min before measuring the pH value. Additional drug was added as necessary. Results are in terms of the free base form of the drug.

Partition Coefficient

The partition coefficient (log *P*) of R1626 was determined at 25°C using the Sirius GLpKa titrator. The general titration method and data analysis are the same as described in section "Dissociation Constant." For log *P* measurement, approximately 4 mg of R1626 was weighed into four titration vials, and 18 mL of 0.15 M KCl aqueous solution was added into each vial. Then, 0.1, 0.2, 0.3, and 0.5 mL of *n*-octanol was added in vials 1–4 accordingly. The sample was titrated from pH 2.0 to 10 with standard 0.5 M HCl and 0.5 M KOH. pK_a values of R1626 were measured in aqueous and in the aqueous/*n*-octanol phases, respectively. The log *P* value was calculated based on the pK_a shifts at different *n*-octanol/aqueous volume ratios.

Permeability by Caco-2 Measurements

Caco-2 Cell Culture

Caco-2 cell monolayers were prepared and provided by Cell Culture Core Facility in Roche Palo Alto. Caco-2 cells were maintained at 37°C in Dulbecco's modified Eagle's medium (DMEM/high) from Gibco Life Technologies (Gaithersburg, MD, USA) with 10% fetal bovine serum, 0.1 mM MEM nonessential amino acids, 2 mM L-glutamine, and 100 U/mL penicillin and 100 U/mL streptomycin in an atmosphere of 5% CO_2 and 90% relative humidity. Cells were grown in T225, Corning Vented Cap/Canted Neck, polystyrene, treated, nonpyrogenic (Corning, NY, USA), and split twice per week at 1:15 split ratio. The cells were plated at a density of 78,000 cells/cm^2 on precollagen-coated Transwell polytetrafluoroethylene (PTFE) membrane filters (12-well Transwell inserts, collagen-coated, PTFE membrane, and 0.4 μm pores from Corning). The media was changed twice per week. The cells were used at passage 110–120. The Caco-2 monolayers were cultured for 21 days before use.

Buffer Preparation

The Kreb–Henseleit buffer was prepared by following the manufacture's instructions. The buffer solution was stored in 4°C and warmed up to 37°C before use. Before the experiment, pH of the Kreb–Henseleit buffer was adjusted to 6.5 (for apical side) and 7.4 (for basolateral).

Dosing Solution Preparation

5.73 mg of R1626 was dissolved in 1 mL of dimethyl sulfoxide (DMSO). 46.3 μL of this solution was diluted to 25 mL using pH 6.5 Kreb–Henseleit buffer. The concentration of the dosing solution is 20 μM.

Apical to Basolateral (A to B)

Caco-2 cells were rinsed with the Kreb–Henseleit buffer. pH 6.5 buffer (0.5 mL) was added to the apical side of cell monolayers and 1.25 mL of pH 7.4 buffer to the basolateral side. Cells were equilibrated in a 37°C incubator under an atmosphere of 5% CO_2 and 90% relative humidity for at least 30 min and then Transepithelial electrical resistance (TEER) was measured. TEER values were between 300 and 500 Ω cm^2. The apical side buffer was then removed and replaced with 0.5 mL of the prewarmed 20 μM R1626 dosing solution. After 30-, 60-, and 90-min time points, the cells were transferred to a new plate that had 1.25 mL prewarmed pH 7.4 buffer solution on the receiver sides. The media from all plates were collected as receiver samples.

During the experiment, cell monolayer integrity was evaluated. Before the study, the TEER was monitored with a Milli-Cell ERS device (Millipore, Marborough, MA, USA). In addition, after 60 min of transport studies, 50 μL of 0.5 mg/mL Lucifer Yellow CH solution was dosed to the apical side of cell monolayers. The cells were incubated for another 30 min and then the receiver samples were collected for fluorescence measurement at excitation and emission wavelengths of 409 and 530 nm, respectively.

Sample Analysis

[$^{13}C^{15}N$]-R1479 was used as internal standard with a concentration of 102 ng/mL. The standards of R1626, R1626 monoester, R1626 diester, and R1479 were prepared by diluting the stock solution with Kreb–Henseleit buffer solution; the final concentrations were from 0.2 to 1,146 ng/mL. The samples were acidified to pH 5 and analyzed by reverse-phase HPLC MS methodology on a Thermo Hypersil-Keystone Aquasil C18 column using a 0.1% formic acid-methanol gradient and electrospray ionization on an MSD SCIEX API-4000 mass spectrometer.

Data Analysis

The dQ/dt of test substance was calculated from sampling data at 30, 60, and 90 min. The apparent permeability coefficient (P_{app}) was calculated from the following equation:

$$P_{app} = \frac{dQ}{dt} \times \frac{1}{A \times C_0}, \quad (1)$$

where dQ is the change in total amount of R1626, R1626 diisobutyrate ester, R1626 monoisobutyrate ester, and R1479 in the receiver; A is the surface area (cm^2) of the insert; C_0 is the initial concentration of drug substance; and dQ/dt is the change in drug substance amount in the receiver solution over the 90-min incubation time, that is, the slope of the drug substance amount in the receiver solution versus time.

Chemical Reactivity

Reaction solutions of R1626 at a concentration of approximately 50 μg/mL in 0.001–0.1 N HCl, 0.01 M potassium acetate, 0.01 M potassium phosphate dibasic, and 0.01 M potassium carbonate anhydrous at various pH values were prepared. The ionic strength of the aqueous solutions was adjusted to 0.15 M with potassium chloride.

All sample solutions were flame-sealed into 1 mL clear glass ampoules. Samples of pH 1.05–8.0 were placed in ovens at 40, 50, and 60°C (sample in pH 5.13 was additionally set at 80°C). Samples of pH 9.0–10.85 were placed in ovens at 10°C to 40°C. Several samples at each pH were stored at –20°C to serve as control solutions ("zero time") for the calculation of percentage remaining at the time of assay. At selected time intervals, individual samples were removed from the elevated temperature ovens and stored at –20°C. Samples were allowed to warm to room temperature before analysis by using HPLC. All samples were assayed by using HPLC and the percentage of remaining R1626 was calculated by comparing to –20°C control solutions.

First-order kinetic data for the disappearance of drug were analyzed by fitting the percentage of R1626 versus time to an exponential equation using the data analysis program KaleidaGraph™ (Synergy Software, Reading, PA, USA). pH-rate profile curves were drawn with the smooth function in KaleidaGraph™.

HPLC Methodology

Samples were analyzed by HPLC using the equipment and parameters described in Table 1.

GastroPlus™ Simulations

The percentage absorbed (%F_{abs}) was calculated using the GastroPlus™ software version 5.2.0 from Simulations Plus,

TABLE 1
High-Performance Liquid Chromatography (HPLC)-UV Methodology

Parameter	Description		
Equipment	Waters 2690 or Hewlett Packard 1090		
Column	Zorbax SB-C8, 3.5 μm, 4.6 × 150 mm		
Mobile phase A	20 mM potassium phosphate monobasic pH 2.5		
Mobile phase B	20 mM potassium phosphate monobasic pH 2.5: acetonitrile (20:80)		
Mobile phase flow rate	1.0 mL/min		
Gradient	Time (min)	% A	% B
	0	98	2
	2	98	2
	40	0	100
	44	0	100
	45	98	2
Detection wavelength	270 nm		
Retention time	R1479		5.1 min
	2′-Monoisobutyl ester		12.4 min
	5′-Monoisobutyl ester		13.7 min
	3′-Monoisobutyl ester		14.0 min
	2′,3′-Di-isobutyl ester		21.1 min
	R1626		27 min

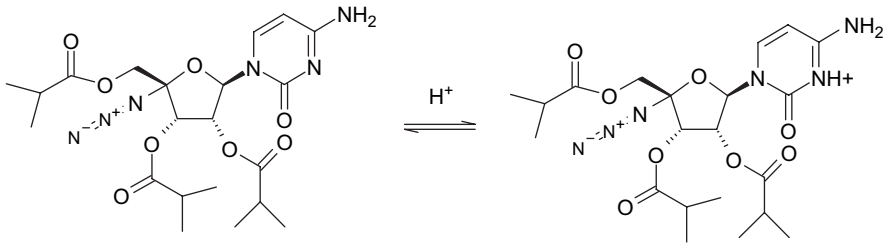

FIGURE 1. Protonation site of R1626.

Inc. (Lancaster, CA, USA). Calculations in GastroPlus™, which uses the Advanced Adsorption and Transit (ACAT) model extended from the work of Yu and Amidon (1999) to describe oral absorption, were done by using physical properties of the drug when known. Default values were used for unknown physical properties and in vivo parameters. Caco-2 values were converted to human effective permeability by using a set of compounds with known effective permeability studied in Caco-2 cells prepared in the same manner as those used in this study. The conversion of Caco-2 value to effective permeability is

$$P_{\text{eff}} = 10^{\,[-0.1264 + 0.5534 \quad \log(\text{Caco-2})\,]}. \tag{2}$$

GastroPlus™ predictions of the $\%F_{\text{abs}}$ were tested by comparing the observed $AUC_{(0\text{–infinity})}$ of R1479 from clinical data (Stella, 2006) at doses ranging from 500 to 12,000 mg R1626 with a predicted AUC, using the equation

$$AUC_{\text{dose}} = AUC_{500\,\text{mg}} \times \text{Dose, mg}/500\,\text{mg} \times \%F_{\text{abs (dose)}}/\%F_{\text{abs (500 mg)}}. \tag{3}$$

This analysis assumes that pharmacokinetics of R1479 is proportional at all doses and that the AUC depends on the fraction absorbed.

RESULTS AND DISCUSSION

Dissociation Constant and Partition Coefficient

R1626 is a cytidine analog that protonates on the cytosine ring (Figure 1). Using potentiometric titration, the dissociation constant was determined in triplicate to be 3.62 ± 0.01 at 25°C and an ionic strength of 0.15 M. The low basicity of the drug limits the number of potential salt forms to those of strong acids such as the hydrochloride salt (Stahl & Nakano, 2002). The strongly acidic nature of the hydrochloride salt in solution suggested protection from water to limit hydrolysis of the ester moieties.

The 1-octanol-water log partition was measured as 2.45 ± 0.02. This value is consistent with a highly permeable drug (Buur, Trier, Magnusson, & Artusson, 1996; Fichert, Yazdanian, & Proudfoot, 2003).

Solubility

The solubility of R1626 (hydrochloride salt) and R1626 (free base) in water was determined to be 10.0 (final pH 1.7) and 0.19 mg/mL expressed as the free base, respectively. Thus, the solubility factor (ratio of the solubility of the salt to the free base) for the GastroPlus™ calculations is 52.

Figure 2 shows the results for pH-solubility studies for R1626. The data were fitted to the equation

$$C = C_{\text{intrinsic}}\left(1+10^{(\text{pKa}-\text{pH})}\right), \tag{4}$$

where C is the equilibrium solubility and $C_{\text{intrinsic}}$ is the solubility of the free base form. The aqueous solubility is pH dependent and decreases with increasing pH (pK_a = 3.62). As the solubility is greater than 100 µg/mL, dissolution is not expected to be present a limit to absorption (Hörter & Dressman, 1997).

Permeability

The Caco-2 model is commonly used to predict drug permeability (Artursson, Palm, & Luthman, 1996; Bailey, Bryla, & Malick, 1996). The effective permeability coefficient of R1626

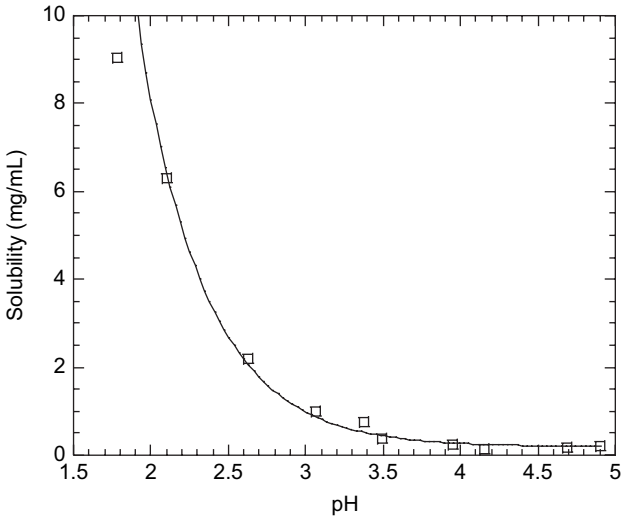

FIGURE 2. pH-solubility profile for R1626.

TABLE 2
Percentage Observed of R1626 Relative to its Di-Isobutyrate, Monoisobutyrate, and R1479 in Transport Studies

Samples	Well 1	Well 2	Average	*SD*
% R1626				
R-30 min	23.41	25.83	24.62	1.71
R-60 min	20.33	21.43	20.88	0.77
R-90 min	13.65	15.12	14.38	1.04
D-0 min	96.95			
D-90 min	67.54	69.37	68.45	1.29
% R1626 di-isobutyrate ester				
R-30 min	55.51	52.13	53.82	2.38
R-60 min	54.24	48.65	51.45	3.95
R-90 min	53.49	51.29	52.39	1.56
D-0 min	2.61			
D-90 min	28.44	27.31	27.88	0.80
% R1626 monoisobutyrate ester				
R-30 min	10.83	10.23	10.53	0.43
R-60 min	13.68	14.70	14.19	0.72
R-90 min	17.31	15.02	16.17	1.62
D-0 min	0.35			
D-90 min	2.28	1.95	2.12	0.24
% R1479				
R-30 min	10.25	11.81	11.03	1.10
R-60 min	11.75	15.22	13.48	2.46
R-90 min	15.55	18.57	17.06	2.14
D-0 min	0.09			
D-90 min	1.74	1.37	1.55	0.26

D, donor; R, receiver.

across 21-day Caco-2 monolayers was determined to be 14.95×10^{-6} cm/s for apical (donor) to basolateral (receiver) direction for the total amount of drug transported at 37°C. The value corresponds to a human effective permeability of 3.3×10^{-4} cm/s (see experimental section) (Artursson et al., 1996; Fichert et al., 2003).

Table 2 summarizes the percentage of R1626, di-isobutyrate, monoisobutyrate, and parent drug at different time points on the donor and receiver sides of the membrane. The percent conversion from tri-isobutyrate to di-isobutyrate is the highest, followed by parent drug and monoisobutyrate. As the mono- and di-isobutyrates and drug present on the receiver side of the membrane would diffuse back to the donor side, the effective permeability coefficient may underestimate the effective permeability. On the basis of the correlation of oral absorption in humans with Caco-2 permeability values reported in the literature (Rubas, Jezyk, & Grass, 1993), R1626 is considered as a highly permeable drug.

Chemical Reactivity

Because of the formulation challenges with ester prodrugs (Strickley & Oliyai, 2007), a pH-rate profile was completed. The kinetics of degradation of R1626 in aqueous solution was determined by following the disappearance of the drug (area of the drug peak compared to a –20°C control sample). The observed first-order rate constants (k_{obs}) for the degradation of R1626 at different temperatures in aqueous solutions are summarized in Table 3. The pH-rate profile for the degradation of the R1626 in aqueous solution at 40, 50, and 60°C is shown in Figure 3. Typical HPLC chromatograms are shown in Figure 4.

The results show that the reaction is catalyzed by both acid and base. The most stable pH for R1626 in aqueous solution

TABLE 3
Observed First-Order Rate Constants for the Degradation of RO4588161 in Aqueous Solution at Different Temperatures

	k_{obs} (day^{-1})							
pH[a]	10°C	20°C	25°C	30°C	40°C	50°C	60°C	80°C
1.05					1.25	2.24	4.29	
2.04					0.11	0.21	0.39	
3.03					0.017	0.036	0.073	
4.02					0.004	0.008	0.018	
5.13					0.0014[b]	0.0044	0.013	0.098
					1			
6.00					0.01	0.028	0.082	
7.10					0.097	0.3	0.8	
8.00					0.68	1.84	5.08	
9.00		0.41		1.31	4.1			
10.00		4.54		13.54	31.74			
10.85	6.54		56.4	65	234.5[b]			

[a]Measured at room temperature.
[b]Extrapolated using the Arrhenius equation.

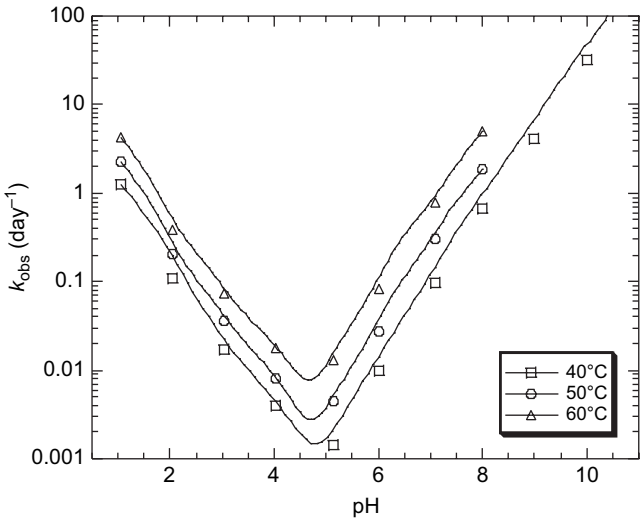

FIGURE 3. pH-rate profiles for the degradation of R1626 in aqueous solution.

is around pH°5. The major degradation products are the diesters of R1626, the monoesters of R1626, and the R1479. Cytosine was found in some chromatograms. Because of the reactivity in water, formulations are protected from exposure to moisture.

Also, the hydrolysis of the prodrug observed in the permeability studies is significantly faster than that observed in the hydrolytic reactivity. For example, after 90 min, the donor and receiver sides have 14.38 and 68.45% R1626, respectively, whereas at pH 6.5 and 7.4 at 40°C, the aqueous half life is greater than 10 and 2 days, respectively. Therefore, the data suggest that the Caco-2 membrane catalyzes the hydrolysis of the prodrug (Imai, Imoto, Sakamoto, & Hashimoto, 2005). The hydrolysis of the R1626 by the intestinal membrane reduces the metabolic complexity of the triester prodrug.

GastroPlus™ Simulations

Physical Property Parameters

Table 4 lists the physical property values used in the GastroPlus™ calculations not previously identified.

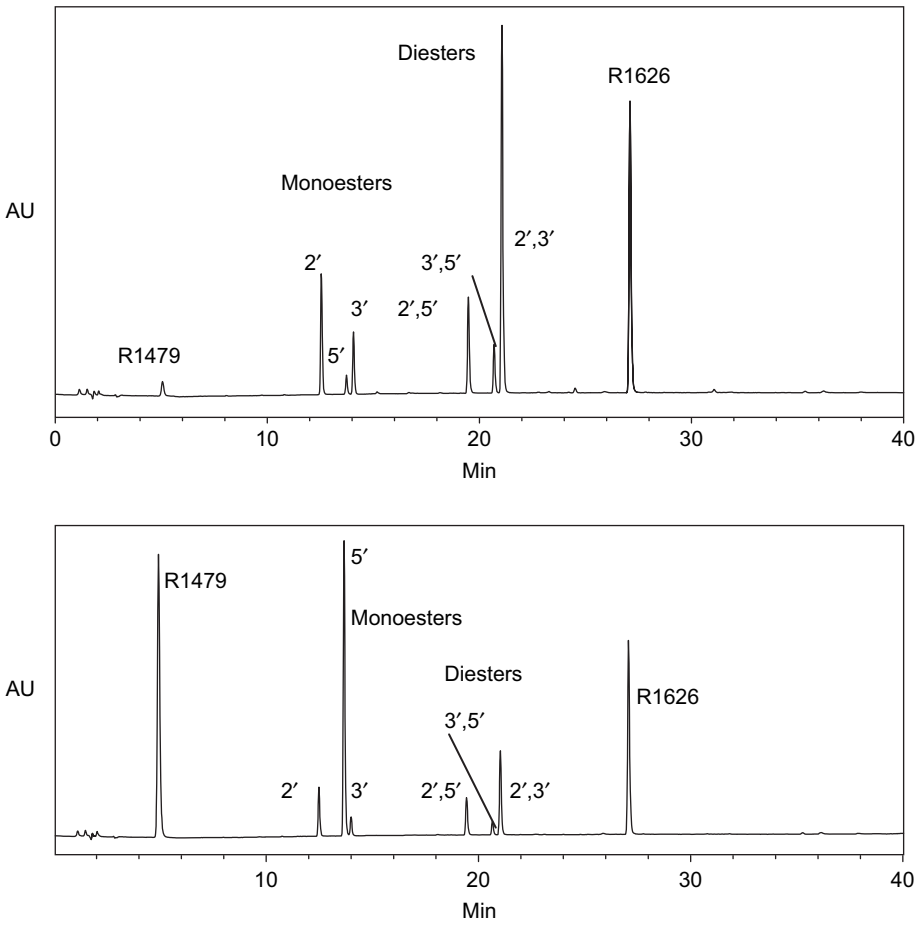

FIGURE 4. Typical high-performance liquid chromatography (HPLC) chromatograms for the degradation of R1626 in pH 2 (top) and pH 5 (bottom) at 50°C after 5 days.

TABLE 4
Physical Properties Used in GastroPlus™ Calculations

Parameter	Value
Molecular weight	494.5 u
Dose volume	250 mL
Diffusion coefficient	0.5875 $cm^2/s \times 10^{5a}$
Drug particle density	1.2 g/mL
Mean precipitation time	900 s
Dosage form	IR tablet
Particle size	5 μm

[a]Calculated based on molecular weight using ADMET Predictor™ from Simulations Plus, Inc.

Prediction of the Effect of Dose

To test the GastroPlus™ model, the ability for it to predict the effect of dose on AUC using clinical tablets (Ahmed et al., 2007) was compared. To convert %*F* values to AUC, it was assumed that the program accurately would predict the %*F* value for the 500-mg dose. GastroPlus™ generally predicts the data very well (Figure 5). At dosing below 6,000 mg, it slightly overpredicts the AUC; at the 12,000-mg dose, it underpredicts the AUC.

A common model for predicting the effect of dose is the maximum absorbable dose (MAD) (Curatolo, 1998; Fagerholm, 2007; Sun et al., 2004). In this model, the MAD is defined as follows:

$$MAD = P_{eff} \quad S \quad 2\pi L \quad T, \tag{5}$$

where P_{eff} is the drug permeability in the human intestine, *S* the aqueous solubility, *L* the length of the small intestine, and *T* the residence time in the small intestine.
Using

- $P_{eff} = 3.3 \times 10^{-4}$ cm/s;
- *S* = 0.19 mg/mL;
- *T* = 180 min for humans.

Thus, the MAD for R1626 is about 5,000 mg. If the effective absorption surface of 800 cm^3 is used (Yu, 1999), an MAD value of about 500 mg is obtained. The high AUC levels at doses greater than the MAD suggest that the drug may have good absorbance throughout the large intestine in addition to the small intestine.

Effect of Particle Size

Particle size is frequently an important parameter for the %*F* of low-solubility drugs (Johnson & Swindell, 1996). Figure 6 shows the effect of particle size on doses of R1626 from 500 mg to 12,000 mg as predicted by GastroPlus™ from 2.5 to 250 μm. The percentage change in $\%F_{abs}$ varies from 13 to 29 and is at a maximum at a dose of 3,000 mg. More importantly, the calculations predict that a variation in particle size less than 25 μm results in a change in $\%F_{abs}$ of 6% or less.

Effect of Solubility and Permeability

As an increase in lipophilicity and the resulting increase in permeability result in an expected decrease in solubility (Ghosh & Mitra, 1991), getting the right balance in lipophicity is important. Table 5 summarizes the relationship between solubility and Caco-2 permeability on the $\%F_{abs}$ calculated by GastroPlus™. The calculations suggest that prodrugs of R1626

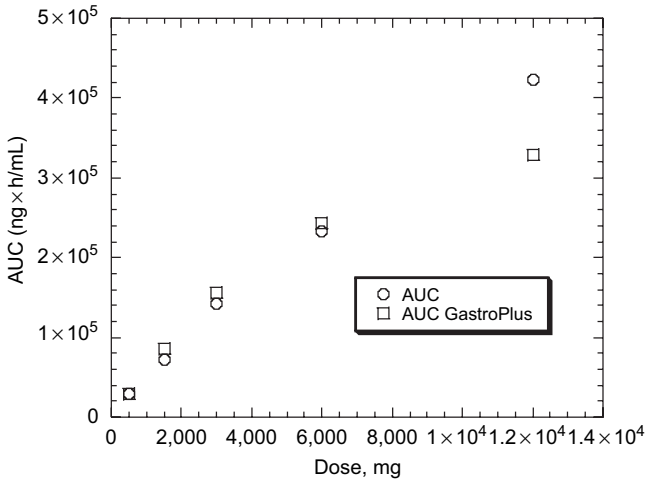

FIGURE 5. Plot of dose versus AUC observed and predicted by using GastroPlus™.

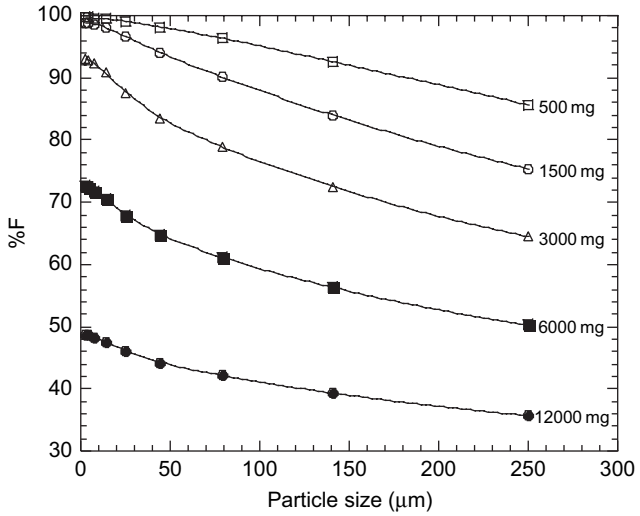

FIGURE 6. Effect of particle size on $\%F_{abs}$ predicted by using GastroPlus™.

TABLE 5
Effect of Solubility and Permeability on % F_{abs} Calculated by GastroPlus™ for a Dose of 1,500 mg

Caco-2 Permeability $\times 10^6$ (cm/s)	0.3				
Simulation $P_{eff} \times 10^4$ (cm/s)	0.3845	1	3	10	30
Solubility (μg/mL)	% F_{abs} predicted	0.7482	1.3736	2.673	4.9097
3	2.2	4.1	7.2	13	20
8	4.8	8.8	15	25	39
19	9.9	18	29	47	69
44	19	33	52	78	96
100	34	56	80	98	99.9
250	56	82	97	100	100
590	79	94	99	100	100
1,400	83	95	99	100	100
3,000	83	95	99	100	100

can be obtained with a modest permeability in the Caco-2 assay of 1×10^{-6} cm/s although a solubility of greater than 250 μg/mL would be required. Similarly if the solubility is less than 44 μg/mL, a high permeability is necessary. Targeting a solubility of greater than 100 μg/mL and Caco-2 permeability greater than 3×10^{-6} cm/s is expected to achieve a high %F_{abs}. The MAD value obtained for this solubility and permeability is about 100 mg.

CONCLUSION

The increase in exposure and dose proportionality for the tri-isobutyrate prodrug over the parent nucleoside can be explained by the high permeability and solubility of the prodrug. In general, targeting Caco-2 permeability and solubility of greater than 3×10^{-6} cm/s and 100 μg/mL, respectively, would be expected to give successful prodrugs for this class of nucleoside prodrug.

ACKNOWLEDGMENTS

The authors thank colleagues at the cell culture, analytical, and mass spectral groups of Roche Palo Alto, the Roche Nutley formulation group, and members of the R1479 and R1626 Research and Development teams for contributions to this article.

REFERENCES

Ahmed, H. A., Alfredson, T. V., Birudaraj, K., Brandl, M. T., Phuapradit, W., Shah, N. H., & Stefanidis, D. (2007). HCV prodrug formulation. *PCT Int. Appl.*, WO2007068615, 15 pp.

Albert, A. (1958). Chemical aspects of selective toxicity. *Nature, 182*, 421–422.

Alfredson, T., Sarma, K., Brandl, M., Larrabee, S., Wu, X., Tu, Y., et al. (2006). Design and evaluation of novel HCV Polymerase inhibitor prodrugs with enhanced oral bioavailability. *AAPS Annual Meeting and Exposition*, (Poster M1214), San Antonio, TX.

Artursson, P., Palm, K., & Luthman, K. (1996). Caco-2 monolayers in experimental and theoretical predictions of drug transport. *Adv. Drug Deliv. Rev., 22*, 67–84.

Avdeef, A. (2001). Physicochemical profiling (solubility, permeability and charge state). *Curr. Top. Med. Chem., 1*, 277–351.

Bailey, C. A., Bryla, P., & Malick, A. W. (1996). The use of the intestinal epithelial cell culture model, Caco-2 in pharmaceutical development. *Adv. Drug Deliv. Rev., 22*, 85–103.

Beaumont, K., Webster, R., Gardner, I., & Dack, K. (2003). Design of ester prodrugs to enhance oral absorption of poorly permeable compounds: Challenges to the drug discovery scientist. *Curr. Drug Metab., 4*, 461–485.

Buur, A., Trier, L., Magnusson, C., & Artusson, P. (1996). Permeability of 5-fluorouracil and prodrugs in Caco-2 cell monolayers. *Int. J. Pharm., 129*, 223–231.

Cho, A. (2006). Recent advances in oral prodrug discovery. *Annu. Rep. Med. Chem., 41*, 395–407.

Curatolo, W. (1998). Physical chemical properties of oral drug candidates in the discovery and exploratory development setting. *Pharm. Sci. Technolo. Today, 1*, 387–393.

Devos, R. R., Hobbs, C. J., Jiang, W.-R., Martin, J. A., Merrett, J. H., Najera, I., Shimma, N., & Nobuo, T. T. (2002). Preparation of 4′-substituted nucleosides as antiviral agents. *PCT Int. Appl.*, WO2002100415.

Di, L., & Kerns, E. H. (2006). Application of physicochemical properties to support lead optimization by discovery teams. In R. T. Borchardt, E. H. Kerns, M. J. Hageman, D. R. Thakker, & J. L. Stevens (Eds.), *Optimizing the "drug-like" properties of leads in drug discovery* (pp. 167–194). New York: Springer.

Ettmayer, P., Amidon, G., Clement, B., & Testa, B. (2004). Lessons learned from marketed and investigational prodrugs. *J. Med. Chem., 47*(10), 2393–2404.

Fagerholm, U. (2007). Prediction of human pharmacokinetics-gastrointestinal absorption. *J. Pharm. Pharmacol., 59*, 905–916.

Fichert, T., Yazdanian, M., & Proudfoot, J. R. (2003). A structure permeability study of small drug-like molecules. *Bioorg. Med. Chem. Lett., 13*(4), 719–722.

Ghosh, M. K., & Mitra, A. K., (1991). Effects of 5′-ester modification on the physicochemical properties and plasma protein binding of 5-iodo-2′-deoxyuridine. *Pharm. Res., 8*(6), 771–775.

Gomez-Orellana, I. (2005). Strategies to improve oral drug bioavailability. *Expert Opin. Drug Deliv., 2*(3), 419–433.

Hageman, M. J. (2006). Solubility, solubilization and dissolution in drug delivery during lead optimization. In R. T. Borchardt, E. H. Kerns, M. J. Hageman, D. R. Thakker, & J. L. Stevens (Eds.), *Optimizing the "drug-like" properties of leads in drug discovery* (pp. 99–130). New York: Springer.

Ho, N. F. H., Park, J. Y., Morozowich, W., & Higuchi, W. T. (1976). Physical model approach to the design of drugs with improved intestinal absorption. In E. B. Roche (Ed.), *Design of biopharmaceutical properties through prodrugs and analogs* (pp. 136–217). Washington, DC: American Pharmaceutical Association.

Hörter, D., & Dressman, J. (1997**).** Influence of physicochemical properties on the dissolution of drugs in the gastrointestinal tract. *Adv. Drug Deliv. Rev., 25*, 3–14.

Imai, T., Imoto, M., Sakamoto, H., & Hashimoto, M. (2005). Identification of esterases expressed. In Caco-2 cells and effects of their hydrolyzing activity in predicting human intestinal absorption. *Drug Metab. Dispos., 33*(8), 1185–1190.

Johnson, K. C., & Swindell, A. C. (1996). Guidance in the setting of drug particle size specifications to minimize variability in absorption. *Pharm. Res., 13*(12), 1795–1798.

Klumpp, K., Leveque, V., Le Pogam, S., Ma, H., Jiang, W.-R., Kang, H., Granycome, C., Singer, M., Laxton, C., Hang, J. Q., Sarma, K., Smith, D. B., Heindl, D., Hobbs, C. J., Merrett, J. H., Symons, J., Cammack, N., Martin, J. A., Devos, R., & Najera, I. (2006). The novel nucleoside analog R1479 (4′-azidocytidine) is a potent inhibitor of NS5B-dependent RNA synthesis and hepatitis C virus replication in cell culture. *J. Biol. Chem., 281*(7), 3793–3799.

Li, F., Maag, H., & Alfredson, T. (2008). Prodrugs of nucleoside analogues for improved oral absorption and tissue targeting. *J. Pharm. Sci., 97*, 1109–1134.

Mackman, R. L., & Cihlar, T. (2004). Prodrug strategies in the design of nucleoside and nucleotide antiviral therapeutics. *Annu. Rep. Med. Chem., 39*, 305–321.

Poijärvi-Virta, P., & Lönnberg, H. (2006). Prodrug approaches of nucleotides and oligonucleotides. *Curr. Med. Chem., 13*, 3441–3465.

Roberts, S., Cooksley, G., Shaw, D., Berns, H. K., Brandl, M. T., Fettner, S. H., Hill, G., Ipe, D., Klumpp, K., Mannino, M., O'Mara, E., Tuo, Y. & Washington, C. B. (2006). Interim results of a multiple ascending dose study of R1626, a novel nucleoside analog targeting HCV polymerase in chronic HCV patients *Journal of Hepatology, 44* (Suppl. 2), S269.

Robson, R., Berns, H., Brandl, M., Fettner, S., Hill, G., Ipe, D., Love, J., Mannino, M., O'Mara, E., Tu, Y., & Washington, C. (2007). Safety, tolerability and pharmacokinetics of R1626, a novel nucleoside analog targeting HCV polymerase: Results from a phase 1 single dose escalation trial in healthy subjects. *Clin. Pharmacol. Ther., 81*(Suppl. 1), S98.

Rubas, W., Jezyk, N., & Grass, G. M. (1993). Comparison of the permeability characteristics of a human colonic epithelial (Caco-2) cell line to colon of rabbit, monkey, and dog intestine and human drug absorption. *Pharm. Res., 10*, 113–118.

Shim, J. H., Hong, Z., & Wu, J. Z. (2006). Recent patents on nucleoside and nucleotide inhibitors for HCV. *Recent Patents Antiinfect. Drug Discov., 1*(3), 323–331.

Smith, D. B., Martin, J. A., Swallow, S., Smith, M., Kaiser, A., Yee, C., Crowell, M., Kim, W., Sarma, K., Najera, I., Jiang, W.-R., Le Pogam, S., Rajyaguru, S., Klumpp, K., Leveque, V., Ma, H., Tu, Y., Chan, R., Brandl, M., Alfredson, T., Wu, X., Birudaraj, R., Tran, T., & Cammack, N. (2006). *From R1479 to R1626: Optimization of a nucleoside inhibitor of NS5B for the treatment of hepatitis C*. Abstracts of papers, 232nd ACS National Meeting, San Francisco, CA, USA, Sept. 10–14.

Stahl, P. H., & Nakano, M. (2002). Pharmaceutical aspects of the drug salt form. In P. H. Stahl & C. G. Wermuth (Eds.), *Handbook of pharmaceutical salts properties, selection and use* (pp. 117–134). Weinheim, Germany: Wiley-VHC and Zürich, Switzerland: Verlag Helvetica Acta.

Stanczak, A., & Ferra, A. (2006). Prodrugs and soft drug. *Pharmacol. Rev., 58*, 599–613.

Stella, V. J. (2006). Prodrug strategies for improving drug-like properties. In R. T. Borchardt, E. H. Kerns, M. J. Hageman, D. R. Thakker & J. L. Stevens (Eds.), *Optimizing the "drug-like" properties of leads in drug discovery* (pp. 221–242). New York: Springer.

Stella, V. J. (2007). Prodrug approaches to enhancing the oral delivery of poorly permeable drugs. In V. J. Stella, R. T. Borchardt, M. J. Hageman, R. Oliyai, H. Maag, & J. W. Tilley (Eds.) *Prodrugs: Challenges and rewards part 1* (pp. 33–82). New York: Springer Sciences.

Stella, V. J., Charman W. N. A., & Naringrekar, V. H. (1985). Prodrugs. Do they have advantage in clinical practice? *Drugs, 29*, 455–473.

Strickley, R. G., & Oliyai, R. (2007). Formulation challenges of prodrugs. In V. J. Stella, R. T. Borchardt, M. J., Hageman, R. Oliyai, H. Maag, & J. W. Tilley (Eds.), *Prodrugs: Challenges and rewards part 2* (pp. 383–410). New York: Springer Sciences.

Sun, D., Yu, L. X., Hussain, M. A., Wall, D. A., Smith, R. L., & Amidon, G. L. (2004). In vitro testing of drug absorption for drug 'developability' assessment: Forming an interface between in vitro preclinical data and clinical outcome. *Curr. Opin. Drug Discov. Devel., 7*(1), 75–85.

Ungel, A.-L., & Abrahamsson, B. (2001). Biopharmaceutical support in candidate drug selection. In Gibson, M. (Ed.), *Pharmaceutical preformulation and formulation a practical guide from candidate drug selection to commercial dosage form* (pp. 97–143). Boca Raton, FL: Taylor and Franci Group.

Yu, L. X. (1999). An integrated model for determining causes of poor oral drug absorption. *Pharm. Res., 16*(12), 1883–1887.

Yu, L. X., & Amidon, G. L. (1999). A compartmental absorption and transit model for estimating oral drug absorption. *Int. J. Pharm., 186*(2), 119–125.